Available online at www.sciencedirect.com

ScienceDirect

Energy Procedia 74 (2015) 507 – 517

Energy Procedia

International Conference on Technologies and Materials for Renewable Energy, Environment and Sustainability, TMREES15

Distributed Photovoltaic Architecture for HVDC-bus Feeding with a Simple Evaluation of Optimal Tracking

H. Allouache[a], A. Zegaoui[a,b], M. Arab[a], B. Belmadani[a], M. Aillerie[b,c]

[a]*UHBC University-Electrotechnic Departement, GEER Laboratory, Hay Essalam 02000 Chlef, Algeria*
[b]*Université de Lorraine, LMOPS-EA 4423, 2 rue Ed. Belin, 57070 Metz, France.*
[c]*CentraleSupelec, LMOPS, 57070 Metz, France.*

.Abstract

This contribution describes, compares, and analyses two structures and their operating modes dedicated to renewable energy production from photovoltaic (PV) sources. Between the two different technical approaches, photovoltaic sources placed in a distributed architecture supplying a high DC voltage HVDC bus points large advantages. Thus, after preliminary comparison of both solutions and concluding phases, this efficient solution finally constitutes the main original analysis presented in this contribution. The distributed PV structure is investigated, implemented and simulated in an original way under the OrCAD/Pspice software environment. The adaptation stage for maximum power transfer is modelled in detail. A method to calculate the optimal duty cycle for optimal use of PV panels power is proposed, tested and validated by the use of a marketed PV module datasheet.

Peer-review under responsibility of the Euro-Mediterranean Institute for Sustainable Development (EUMISD)

Keywords: Photovoltaic modelling; Hidh voltage direct current bus (HVDC-bus); bosst converter; Maximum power point tracking

1. Introduction

Basic photovoltaic (PV) generator (PVG) consists of modules connected in series or in parallel, and a load (continuous load or battery), which uses the produced energy, directly or via an energy transfer by a grid as represented in Fig. 1.

Currently, in such system, the load imposes the operating point and the load current is highly dependent on the intensity of illumination for a given temperature and the value, the nature resistive, inductive or capacitive of the load. Fig. 2 presents several operating points imposed by different resistor-loads in both current-voltage (I-V) and power-voltage (P-V) characteristics. The simulation is made for a given illumination and temperature using the technical characteristics extracted from the panel datasheet of the commercial solar module ESM80S-125, having a

Peer-review under responsibility of the Euro-Mediterranean Institute for Sustainable Development (EUMISD)
doi:10.1016/j.egypro.2015.07.736

maximum peak power of 80Wc within a voltage of 17.6V and current of 4.55 A at the maximum power point (MPP).

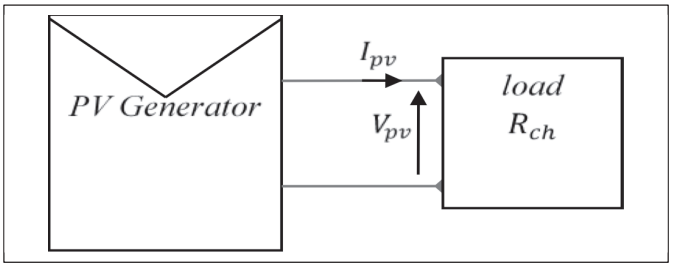

Fig. 1. The basic PV architecture network

In Ref. [1], P. Petit et al. have suggested the use of dedicated converters fed by a distributed photovoltaic architecture connected to HVDC bus, allowing the smart grid approach. Thus, in Ref. [2], same authors have presented new individual DC/HVDC converters dedicated to renewable sources with output voltages in the range 200 Volts up to 1 kVolts adapted to their connection on a common distributed bus. These converters are based on a magnetically coupled boost with a recovery stage allowing a high conversion ratio, a low voltage on the switch, a recovery of the energy losses in the leakage inductors and finally a high conversion efficiency even when HVDC is concerned by the output.

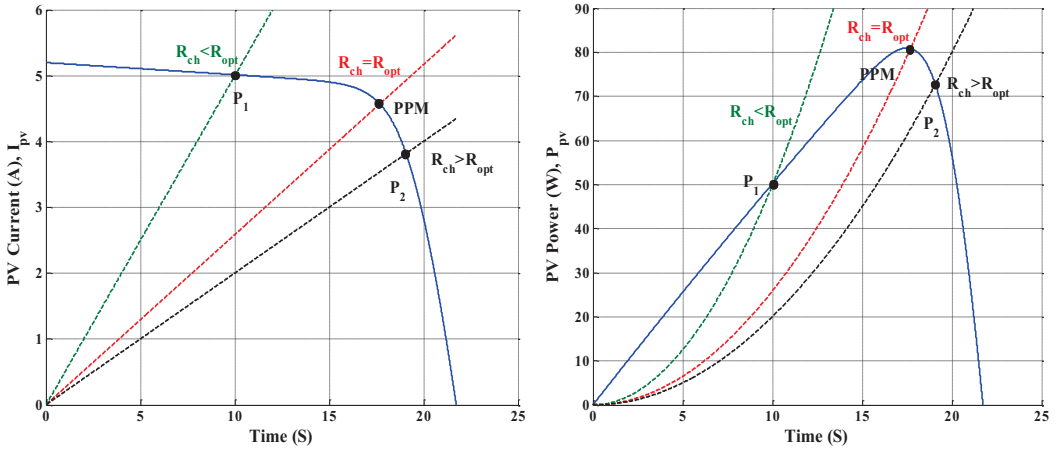

Fig. 2. I-V and P-V characteristics for several operating points.

Unfortunately, the classical modeling of PV systems under various software environments, models are often limited to PV voltages below 200 Volts. For PV panel modeling, mathematical simulations are generally based on current-voltage relationships deduced from the well known single diode model [3, 5], and the five parameters of this model are widely discussed, as example in Refs. [6, 7]. In addition, some authors developed circuit-based piecewise linear PV device model for electronic simulation software after simulations of the current – voltage relationship of the single diode model, done under EMTDC/PSCAD environment [8].

Finally, we note that a new model, named DRM was developed to take into account the reverse mode biasing of PV cells [9, 10]. The most popular models in literature are made to produce behavior of module and are not able to that for high voltage PV panels' configuration. For all these reasons, designers need a reliable and flexible tool for

predicting the electrical characteristics of PV cells, panels and arrays allowing the optimization of the efficiency of the installation considering various sizes and powers for the generator in agreement with the needs. In Ref. [11], we have already presented a single diode model taking into account the characteristic of PV solar cells, developed under Orcad-capture software and expanded to PV module and PV array, which considers a possible output voltage exceeding one kilovolt. Modules are taken in series connection and simulation results are experimentally compared to manufacturer modules.

In the present contribution, we develop an original method allowing the calculation of an optimal duty cycle of the switch of the converter in order to control stage adaptation according to PV generator impedance and load impedance. Within original implementation under Orcad/Pspice software environment, the value of the calculate duty cycle of the switch is optimized for a system PVG-Boost-Load and results are faced with the functioning characteristics of a commercial system.

2. Studied PV system to supply PV-HVDC bus

In order to extract maximum power from a PVG at given environmental conditions, PVG should always operate at its maximum power point, MPP as represented in Fig. 2. This MPP can be reached by inserting an impedance adaptation stage. In our case, the adapting stage is a DC-HVDC boost converter, Fig. 3, which fulfills the distributed architecture of the HVDC PV bus. In Fig. 3, the load R_{ch} represents the HVDC bus.

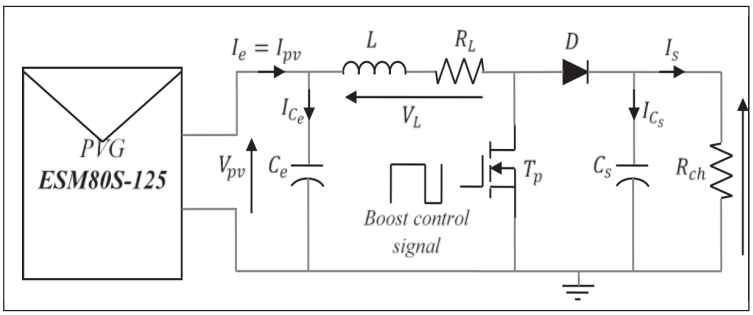

Fig. 3. PVG-boost-Load for distributed PV-HVDC network.

3. Boost in continuous conduction-operating mode (CCM)

The boost operates in CCM operating mode when current through the inductor L cannot be canceled. In this operating mode with the presence of Ce and Cs capacitors, Fig. 4 shows the control signal shape, output voltage Vs(t), inductor current IL(t) , drain MOSFET current ID(t) and voltage across inductor terminals VL(t).

When operating, the average voltage V_{Lmoy} across the inductance must be zero; so according to the areas law we can write:

$$V_s = \frac{V_{pv}}{1-\alpha} \tag{1}$$

Where $0 \leq \alpha \leq 1$ is the duty cycle of the control signal. We can easily deduce that:

$$I_s = (1-\alpha).I_{pv} \tag{2}$$

With $Y = \frac{V_s}{V_{pv}}$, Eq.1 becomes :

$$Y = \frac{1}{1-\alpha} \tag{3}$$

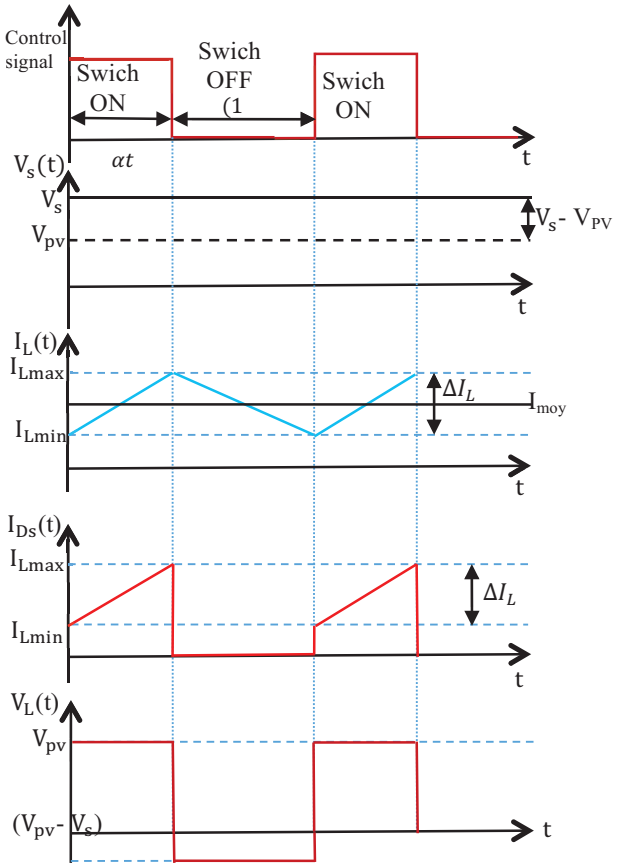

Fig. 4. Control signal and waveform of different instantaneous electric quantities in the boost DC-DC converter operating in CCM with presence of the capacitors

Eq. 2 illustrates that this ratio is constant for a given duty cycle. This is the CCM operating mode.

Ones filtered by Cs capacitor, the output voltage presents ripples. During the switch off time, $(0 < t < \alpha T)$, we can write:

$$V_L = V_{pv} = L\frac{dI_L}{dt} \tag{4}$$

and the ripple current in the inductor is then :

$$\Delta I_L = \alpha\frac{V_{pv}}{L.f} \tag{5}$$

With $f = \frac{1}{T}$ is the switching frequency.

The shapes of the inductor current I_L, diode current I_D and output I_S are reported in Fig. 05.

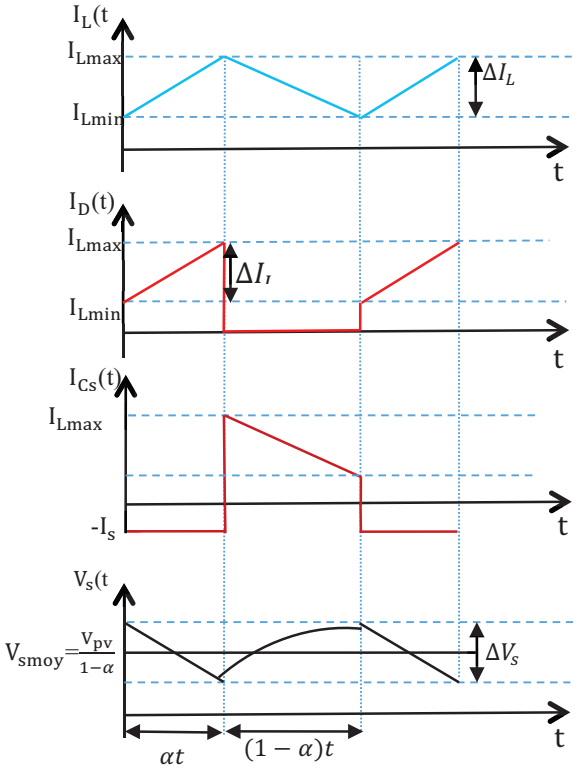

Fig. 5. Wave forms of inductor current IL, diode current ID, Cs capacitor current ICs, output current Is and the output voltage ripples Vs(t).

The ripple voltage is obtained from the differential equation governing the output voltage V_S and by the capacitor current I_{Cs}:

$$V_s = \frac{1}{C_s}\int I_{cs}\,dt + V_{s_0} = \frac{1}{C_s}\int (I_D - I_s)dt + V_{s_0} \tag{6}$$

During switching-off period, the capacitor C_S discharges through the load R_{ch} while the diode is off. By else, the switch being HF controlled, the discharge phase of the capacitor is more rapid yielding to a current I_{Cs} quasi-constant. Since the variation of V_s is linear, the ripple voltage ΔV_s can be written as:

$$\Delta V_s = \left|V_s(t = \alpha T) - V_{s_0}\right| = \frac{I_s}{C_s}\alpha T = \frac{I_s}{C_s}.\frac{\alpha}{f} \tag{7}$$

Where T is the switching period, f the switching frequency, V_{S0} is the initial value of the output voltage and α the duty cycle. Therefore, for a fixed value of a ripple output voltage, capacitor value is sized by:

$$C_s > \frac{I_s}{\Delta V_s f}\alpha \tag{8}$$

Also and as indicated in Fig. 5, the inductor current is the sum of a DC component I_{Lmoy} equal to the input current I_{pv} and a second AC component I_{Lalt} (triangular signal):

$$I_L = I_{Lmoy} + I_{Lalt} = I_{pv} + I_{Lalt} \tag{9}$$

In Refs.[6, 7] authors have analyze the input ripple considering that the current delivered by the generator is almost constant (current source). In our case, this assumption is quite rigorous as the PV generator is not linear. The current I_{pv} may be subject to ripples due to voltage fluctuations of V_{pv}. These current undulations can be minimized by a judicious choice of the Ce capacitor. As part of our simulations, the current through Ce capacitor is given by

$$I_{ce} = I_{pv} - I_L \tag{10}$$

In Fig. 6, we report the inductor current shape and from Eq. 7, we deduce the shape of the capacitor current. The ripple voltage is derived from the differential equation governing voltage and current in the capacitor. We can write:

$$V_{pv} = \frac{1}{C_e}\int I_{ce}\,dt + V_{pv_0} = -\frac{1}{C_e}\int I_{Lalt}\,dt + V_{pv_0} \tag{11}$$

Where V_{PVo} is the initial value of the PV voltage.

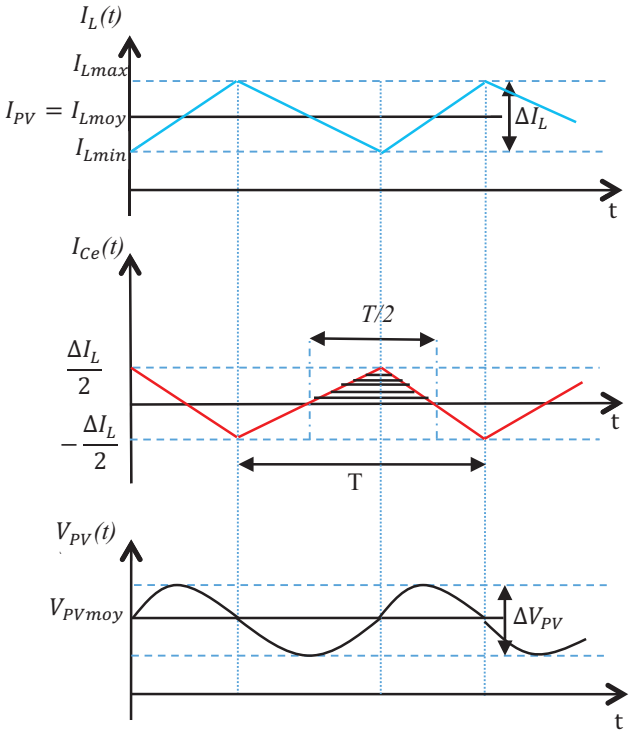

Fig. 6. Wave forms for inductor current, C_e capacitor current waveforms and input voltage V_{PV} ripples.

Integration of Eq. 12 on a half period (see Fig. 6), allows us to evaluate the ripple ΔV_{pv} of the input voltage. This integral is equal to the area of the hatched triangle in figure 06 [8]:

$$\Delta V_{pv} = \frac{1}{C_e}\left(\frac{1}{2}.\frac{T}{2}.\frac{\Delta I_L}{2}\right) = \frac{\alpha V_{pv}}{8.L.C_e.f^2} \tag{12}$$

At fixed ripple output voltage, the value of the input capacitor is

$$C_e > \frac{\alpha}{8.L.f^2}.\frac{1}{\frac{\Delta V_{pv}}{V_{pv}}} \tag{13}$$

4. Impedance adaptation conditions for optimal duty evaluation

According to Eqs. 1 and 2 in CCM mode, we can deduce the expression of the resistor R_{pv} at the output of PV panel as

$$R_{pv} = \frac{V_{pv}}{I_{pv}} = (1-\alpha)^2 R_{ch} \tag{14}$$

Finally:

$$R_{ch} = \frac{R_{pv}}{(1-\alpha)^2} \tag{15}$$

Then, the duty cycle as function of PV panel resistor and load resistor can be easily deduced as

$$\alpha = 1 - \sqrt{\frac{R_{pv}}{R_{ch}}} \tag{16}$$

Since the duty ratio α is less than 1 (α <1), Eq. 16 shows that the converter act as voltage elevator if the Rch load satisfies the following condition

$$R_{ch} > R_{pv} \tag{17}$$

In the case of the marketed PV panel ESM80S-125, at 25°C and when solar illumination varies from 100 to 1000 W/m², the PV panel optimal resistor varies from 51.6 Ω to 3.8 Ω respectively. Therefore, Rch, load resistor must be greater than these values function of the environmental conditions.

By analyzing Eq. 14 and acting that the duty cycle assume the impedance adaptation allowing maximum power transfer, thus, under NTC and for a given load resistor R_{ch}, the optimum value R_{opt} for R_{PV} corresponding to an optimal duty cycle value α_{opt} should obey to the relationship:

$$R_{opt} = \left(1-\alpha_{opt}\right)^2 R_{ch} \tag{18}$$

resulting in a final functioning equation

$$\alpha_{opt} = 1 - \sqrt{\frac{R_{opt}}{R_{ch}}} \tag{19}$$

5. Simulations and results

Simulations were performed under Orcad/Pspice software environment. Fig. 7 shows the studied system implemented under Orcad.

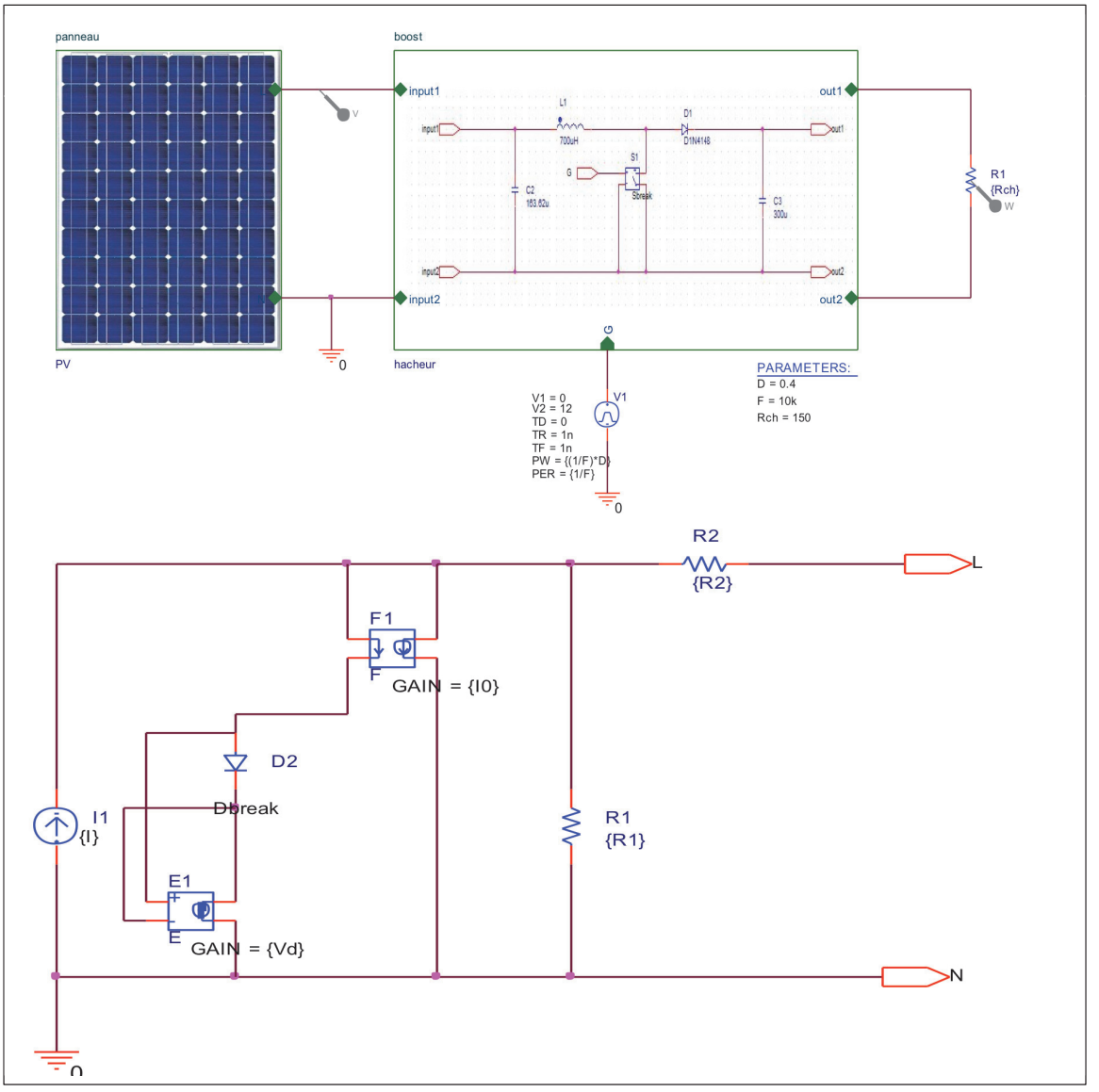

Fig. 7. Studied system implemented under Orcad software and the original implementation of PV Panel.

Simulations were performed under a constant illumination of 1000W/m², a constant temperature of 25°C. The load connected to the boost is a resistive load Rch = 50Ω. In these conditions, a maximum duty cycle α = 0.7226 is calculated according to equation 20. The temporal analysis allowed us to obtain the typical results of power, voltage and current in both boost input and output. Simulation results are presented in figures 08, 09 and 10.

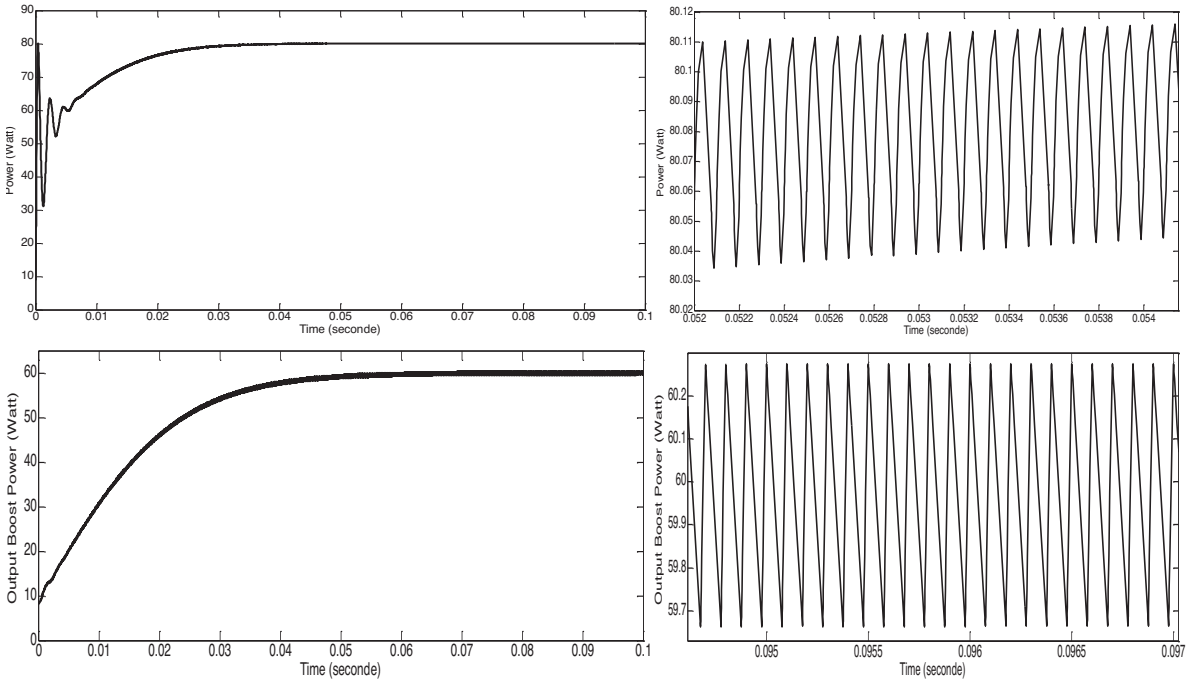

Fig. 8. PV panel power Ppv and Output boost power versus time for $\alpha = 0.7226, R_{ch} = 50\Omega,\ solar\ irradiation\ of\ 1000W/m^2 at\ 25°C$.

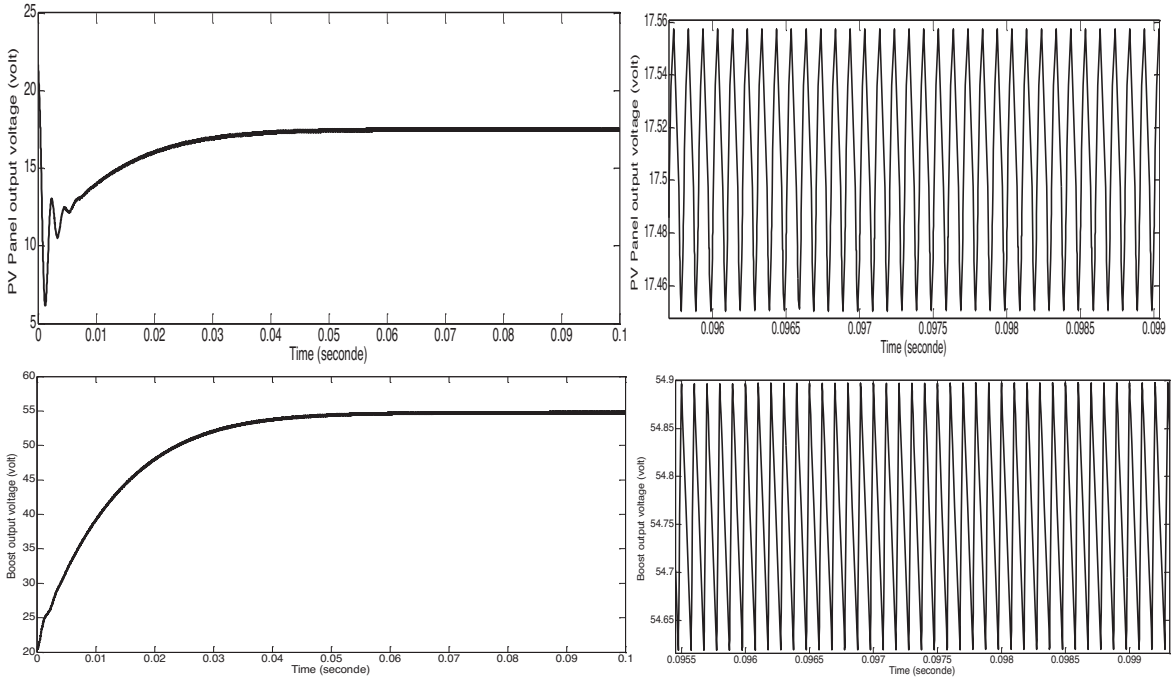

Fig. 9. PV panel voltage Vpv and Output boost voltage versus time for $\alpha = 0.7226, R_{ch} = 50\Omega,\ solar\ irradiation\ of\ 1000W/m^2 at\ 25°C$.

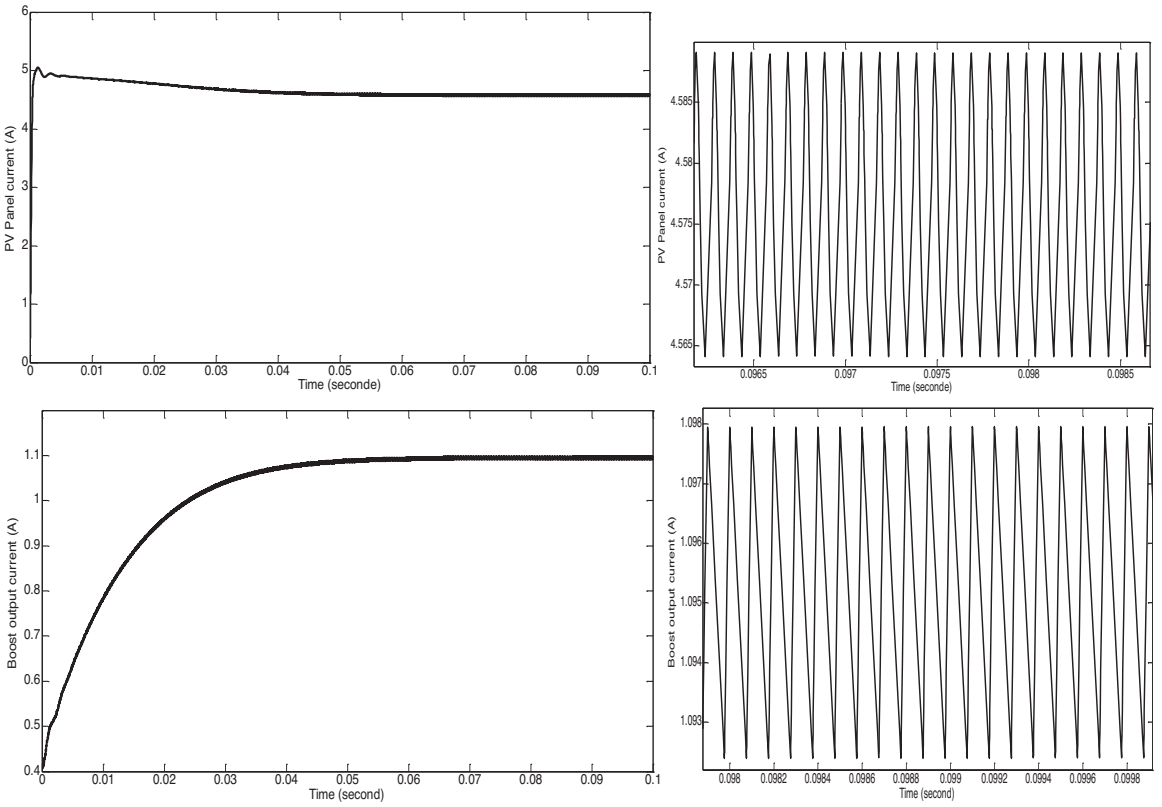

Fig. 10. PV panel current Ipv and Output boost current versus time for $\alpha = 0.7226, R_{ch} = 50\Omega,\ solar\ irradiation\ of\ 1000W/m^2 at\ 25°C$.

After a transient regime of 35 ms at the beginning of the conversion, the steady state is reached. The voltage stabilizes at the values of 17.5V in the boost input and 61V at its output. this refers to the boost function. By the presence of Cs the filtering capacitor, the output voltage stabilizes around the average values of 17.5 V and 61 V. In the steady state, the current is stabilized at the values of 4.65A in the boost input and 1.22A output according to the above equations. The input power (output) is stabilized at 80W (75W). In this case, the efficiency of the boost converter is about of 93.75%. Losses of power (5W) (or 6.25%) are assigned largely to conduction and switching losses in the MOS transistor, by conduction losses in the freewheel diode and magnetic losses in the inductor.

6. Conclusion

The charge adaptation between load and boost converter is a necessary condition for optimal and efficient use of PVs generators (PVG). The boost is a static converter, which accomplishes stage adaptation and allows with a good sizing an increase in voltage at a desired nominal level. The nominal voltage levels expected for the HVDC bus determine the sizing of the different boost components (inductors and capacitors). This method presented in this contribution allows calculating the optimal duty of any marketed PV panel. An original implementation under Orcad/Pspice software environment of a renewable energy generator constituted by PV panels and DC-HVDC boost adapted for providing electrical power to a load is described. Simulations results are within a good agreement with those indicated in the datasheet of the PV panel. The original method applied in the current study point out his efficiency to obtain an easy optimization of the duty cycle allowing an optimal power extraction from PV generator. Finally, the method is completed by experimental results obtained by the Orcad electronic simulated system

allowing an evaluation of the total power losses that occur in a renewable energy generator based on a distributed photovoltaic architecture for HVDC-bus.

References

[1] Petit P., Aillerie M., Sawicki J.P, and Charles J.P. High efficiency DC-DC converters including a performed recovering leakage energy switch. Energy Procedia 2013; 36:642-649.
[2] Petit P., Aillerie M. Integration of individual DC/DC converters in a renewable energy distributed architecture. IEEE:ICIT 2012, , 2012; 802-807.
[3] Chan D.S.H., Phang J.C.H. Analytical methods for the extraction of solar-cell single- and double-diode model parameters from I − V characteristics. IEEE Transactions on Electron Devices 1987; 34:286-293.
[4] Duffie J.A., Beckman W.A. Solar Engineering of Thermal Processes, second ed. John Wiley & Sons Inc., New York. 1991.
[5] Nelson J. The Physics of Solar Cells. Imperial College Press, London. 2003.
[6] Desoto W., Klein S., and Beckman W. Improvement and validation of a model for photovoltaic array performance. Solar Energy 2005; 80:78-88.
[7] Rajapakse A.D., Muthumuni D. Simulation tools for photovoltaic system grid integration studies. IEEE:Electrical Power Energy Conference (EPEC), 2009; 1-5.
[8] Campbell R.C. A circuit-based photovoltaic array model for power system studies. 2007 39th North American Power Symposium, 2007; 97-101.
[9] Zegaoui A., Petit P., Aillerie M., Sawicki J.P., Belarbi A.W., Krachai M.D., and Charles J.P. Photovoltaic Cell /Panel/Array Characterizations and Modeling Considering Both Reverse and Direct Modes. Energy Procedia 2011; 6:695-703.
[10] Zegaoui A., Aillerie M., Petit P., Sawicki J.P., Charles J.P., and Belarbi A.W. Dynamic behaviour of PV generator trackers under irradiation and temperature changes. Solar Energy 2011; 85:2953-2964.
[11] Zegaoui A., Allouache H., Kellal M., Arab M., Bachir G., and Aillerie M. Modeling of the Characteristics of Photovoltaic Sources Feeding a HVDC Bus, Energy Procedia 2014; 50:437-444.